Mar Geophys Res (2011) 32:207–223
DOI 10.1007/s11001-011-9135-z

ORIGINAL RESEARCH PAPER

GIS-based mapping for marine geohazards in seabed fluid leakage areas (Gulf of Cadiz, Spain)

Ricardo León · Luis Somoza

Received: 11 March 2010 / Accepted: 3 May 2011 / Published online: 11 June 2011

Abstract This paper applies, for the first time in offshore deepwater, a method based on geographic information systems for seafloor susceptibility assessment as a first approach to marine geohazard mapping in fluid leakage areas (slope instabilities, gas escapes, seabed collapses, pockmarks, etc.). The assessment was carried out in a known seabed fluid-flow province located on the Iberian margin of the Gulf of Cádiz, Spain. The method (based on statistical bivariate analysis) creates a susceptibility map that defines the likelihood of occurrence of seafloor features related to fluid flow: crater-like depressions and submarine landslides. It is based on the statistical index (*Wi*) method (Van Westen in Statistical landslide hazard analysis. ILWIS 2.1 for Windows application guide. ITC Publication, Enschede, pp 73–84, 1997), in which *Wi* is a function of the cartographic density of seafloor features on "factor maps". The factors selected monitor the seafloor's capability to store and transfer hydrocarbon gases and gravitational instability triggers: geology-lithology, gas hydrate stability zone thickness (temperature, pressure–water depth and geothermal gradient), occurrence of diapirs, proximity to faults or lineaments, and slope angle of the seafloor. Results show that the occurrence of seafloor features related to fluid flow is highest where the factors "gas source and storage" and "pathways of fluid escape" converge. This means that they are particularly abundant over diapirs in contourite deposits, in the vicinity of faults, and inside theoretical gas hydrate stability fields thinned by warm undercurrents. Furthermore, the submarine landslides located on the Palaeozoic-Toarcian basement are not related to fluid leakage. This methodology provides helpful information for hazard mitigation in regional selection of potential drill sites, deep-water construction sites or pipeline routes. It is an easily applied and useful tool for taking the first step in risk assessment on a regional scale for vast areas where fluid leakage may be present, the geological model is known, and the geologically hazardous features have already been mapped.

Keywords Susceptibility maps · GIS · Gulf of Cadiz · Marine geohazard

R. León (✉) · L. Somoza
IGME, Geological Survey of Spain, Rios Rosas 23,
28003 Madrid, Spain
e-mail: r.leon@igme.es

Introduction

Seepage-related geomorphic seafloor features are direct indicators of hydrocarbon migration that provide a sign of hydrocarbon potential in deep sediments (Heggland 1998). Fluid expulsion may play a role in potential instabilities on slopes (Prior and Coleman 1984; Evans et al. 1996; Yun et al. 1999; Cochonat et al. 2002) and involve a risk for human activities (Sultan et al. 2001; Elverhøi et al. 2002). Seafloor features on continental margins, such as mud volcanoes, pockmarks, collapses, and hydrocarbon-derived authigenic carbonates (HDACs) are thought to result from the sometimes catastrophic expulsion of large volumes of fluid (Bayon et al. 2007; Gay et al. 2007; Judd and Hovland 2007). Occurrence of these seafloor features is controlled by factors that define the source and storage of fluids and factors that drive their migration. Seafloor features related to fluid leakages indicate areas where the increase in pore pressure due to free gas accumulation in sediment pore spaces decreases the effective stress and shear strength of the sediments and can cause slope failures (e.g. Prior and Coleman 1984; Hovland and Judd 1988; Yun et al. 1999).

The risk analysis considers three phases in the study of geological processes, each implying a higher level of knowledge: predisposition of a seafloor to the occurrence of a given process (susceptibility), probability of occurrence (hazard), and induced economic or human damage (risk) (Ayala et al. 1987). In onshore environments, susceptibility and hazard and risk assessment have become topics of major interest with the development of geographic information system (GIS) techniques for geoscientists, engineering professionals, and managers at a local level (Varnes 1984; Carrara et al. 1991; Lee et al. 2002). Landslide susceptibility may be assessed through heuristic, statistical, and deterministic approaches (Soeters and Van Westen 1996; Van Westen and Terlien 1996).

The aim of this study was to produce susceptibility maps of seafloor features related to fluid flow using the statistical index (*Wi*) method (Van Westen 1997). This paper presents a method based on GIS technologies for susceptibility assessment of potential crater-like depressions and submarine landslides in areas of fluid leakage.

As a case study to apply and validate the presented method, we selected a venting area of the Gulf of Cadiz, the Tasyo field (Somoza et al. 2003), where the oceanic and geologic conditions may promote preferential areas of fluid pathways and potential hydrate dissociation areas. These conditions are: (a) widespread occurrence of hydrocarbon-enriched fluids affecting the seafloor, such as mud volcanoes, pockmark fields, and carbonate chimneys (Baraza and Ercilla 1996; Somoza et al. 2002; León et al. 2006); (b) occurrence of gas hydrates related to high accumulation of hydrocarbon gases in the subsurface, such as diapiric ridges and mud volcanoes (Ivanov et al. 2000; Grevemeyer et al. 2009); and (c) a complex pattern of warm and cold deep-water currents due to the Mediterranean outflow undercurrent that sweeps the seafloor on this part of the continental margin (Ochoa and Bray 1991; Bower et al. 2002) (Fig. 1).

Geologic and oceanic settings

The Gulf of Cádiz is located on the west side of the Alpine-Mediterranean orogenic belt (Fig. 1). The NW–SE African-Eurasian convergence (Platt et al. 2006) caused the westward drift of the Betic-Rifean Arc and the emplacement of huge chaotic masses named the Allochthonous Unit of the Gulf of Cádiz (AUGC), which is responsible for widespread mud and salt diapirism (Maldonado et al. 1999; Fernández-Puga 2004; Medialdea et al. 2004). Diapirs, belonging to the Miocene M1 formation (Maldonado et al. 1999), are composed mainly of cohesive, low-porosity, grey-black marly clays with limestones and plastic and compacted green clays (Maldonado et al. 1999). Major tectonic structures comprise thrust faults, extensional faults, and strike-slip faults, to which diapirism is closely related (Maldonado et al. 1999), revealing an intense activity of seabed fluid flow on both the Iberian and the African margins (Fernández-Puga et al. 2007; Medialdea et al. 2009; León et al. 2006, 2010).

The study area is located in the Tasyo field (Somoza et al. 2003). This province contains numerous seabed fluid flow features such as mud volcanoes, some of them bearing hydrates (Ivanov et al. 2000; Gardner 2001; Somoza et al. 2000, 2003), HDAC chimneys (Díaz-del-Río et al. 2003; Pinheiro et al. 2003) and crater-like depressions (Baraza and Ercilla 1996; León et al. 2006, 2010). A bottom simulating reflector has been observed locally and as discontinuous levels on the Iberian (Somoza et al. 2000; Casas et al. 2003) and Moroccan slopes (Depreiter et al. 2005).

The upper and middle slopes of the Tasyo field are covered by the contourite depositional system (CDS) (Faugères et al. 1984) generated by the Mediterranean outflow water (MOW). The CDS is composed of large, elongated mounded and sheeted contourite drifts that are 10 km long (Faugéres et al. 1984; Habgood et al. 2003; Hernández-Molina et al. 2003) and is a sedimentary stacked Plio-Quaternary sequence that is very well sorted with low cohesion of silty sands and sandy silts. Sandy contourites are less cohesive than clayey sediments and are also susceptible to liquefaction under dynamic loading (Wilson et al. 2003).

In the study area, the (mainly Palaeozoic) basement outcrops locally on the Guadalquivir Bank (Figs. 2, 6a). It is composed of very cohesive wackes similar to the Culm facies of Upper Visean (Carboniferous) age, undated basalts and limestones of probable Toarcian (Early Jurassic) age (Baldy et al. 1977). Intra-slope diapiric basins (Habgood et al. 2003) are located on the lower slope of the study area, and are composed of pelagic sediments and greyish-brown clays that are rich in foraminifera and bioturbated, with a terrigenous admixture and irregular, patchy laminated intervals (Kenyon et al. 2000).

The MOW is a geostrophic undercurrent flowing between 600 and 1,500 m water depth and intercalated between the North Atlantic Deep Water and the North Atlantic Central Water. It warms the seafloor, flowing westward from the Strait of Gibraltar towards San Vicente Cape along several channelled branches (contourite channels, furrows and moats) (Kenyon and Belderson 1973; García et al. 2009) controlled by the positive relief of diapiric ridges (Hernández-Molina et al. 2003). Glacial/interglacial increases in the Mediterranean outflow gave rise to episodic floods of the MOW undercurrent over the Tasyo field, leading to the formation of sedimentary lobes and submarine fans at the ends of the channels that cross this field (Kenyon and Belderson 1973; Habgood et al. 2003).

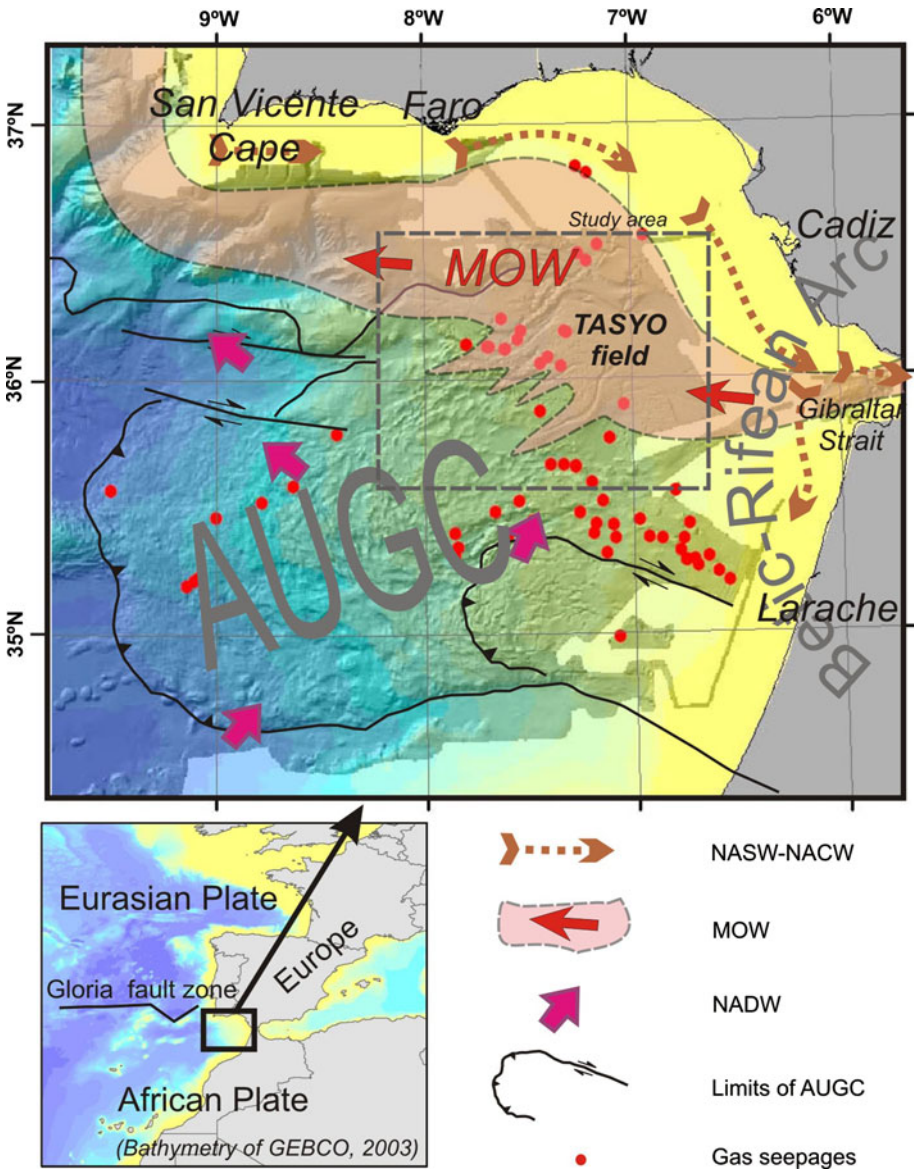

Fig. 1 Geological and oceanographic setting of the Gulf of Cadiz, modified from Medialdea et al. (2009) and data incorporated in the present paper on the bathymetry SWIM compilation of Zitellini et al. (2009). *Dotted line* Tasyo field, *MOW* Mediterranean outflow water, *NASW* North Atlantic Surface Water, *NADW* North Atlantic Deep Water, *NACW* North Atlantic Central Water, *AUGC* Allochthonous unit of the Gulf of Cádiz; 1 limit of the AUGC; 2 mud volcanoes

Data and proposed methodology for susceptibility assessment

Data

In this study, a broad database obtained in the Gulf was used (Fig. 2). Multibeam echo-sounder (MBES) data were acquired aboard the R/V *Hespérides* using a hull-mounted Simrad EM-12S-120 (TASYO 2000 cruise), which enabled simultaneous collection of high-resolution seafloor bathymetry and backscatter data. The Simrad EM-12S-120 operated at a frequency of 13 kHz with 81 beams (swath width of 120°) triggering with pulse lengths ranging from 2 to 10 ms and a vertical resolution of 0.6 m. Regional bathymetric data were collected from the GEBCO Digital Atlas (GEBCO 2003) in order to build the map of slope angle of the seafloor.

The Sparker seismic profiles used in this study (Anastasya-00 cruises) were acquired with an energy source ranging from 3,500 to 7,000 J, a recording length of 2 s two-way travel time and a frequency range of 500 Hz to 4 kHz, providing a medium resolution (1–10 m) and a penetration of 100 to 1,000 m. The TOPAS profiles collected during the TASYO 2000 cruise were obtained with a chirp wavelet at two simultaneous primary frequencies of 15 and 18 kHz, providing a resolution of 0.5–1 m and a maximum penetration of 100 m. Digital data were recorded using Delph2 Triton-Elics software, which made it possible to study certain details with post-processing techniques. Positioning during the swath bathymetry and seismic

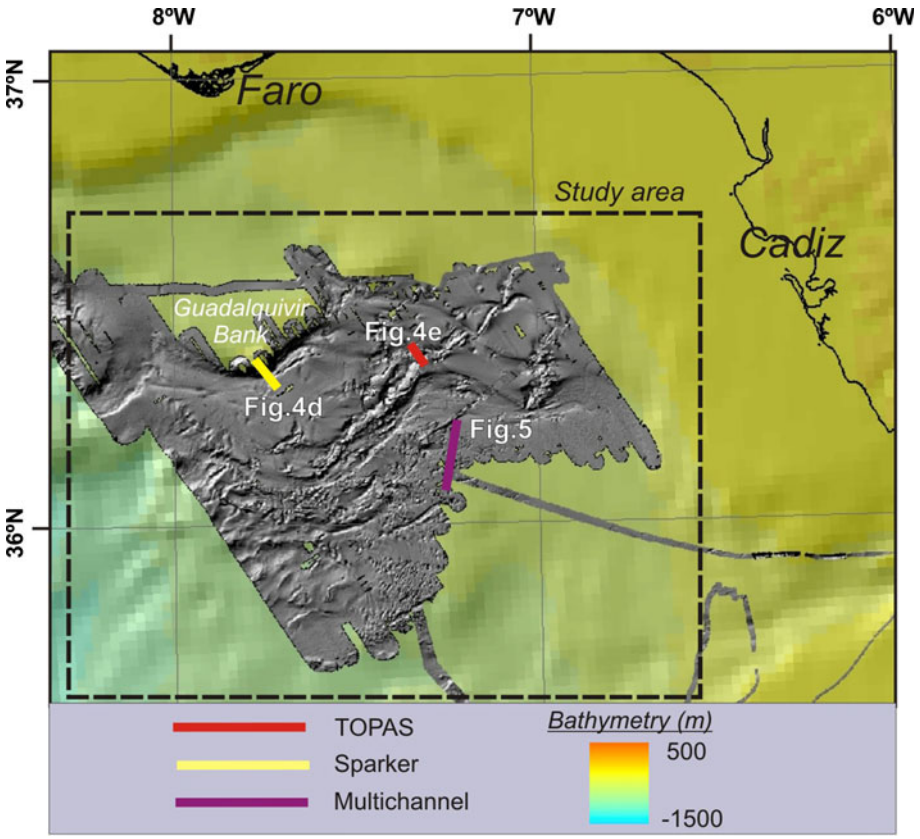

Fig. 2 Datasets used in this paper. Bathymetry compilation from GEBCO (2003) and IGME (2003), Serviços Geológicos de Portugal (1992) and MBES data from Tasyo 2000 cruise. Coloured lines: seismic reflection profiles

cruises was done with Global Positioning System (GPS) and differential GPS techniques.

Proposed methodology for susceptibility assessment

The proposed methodology analyzes the geologic hazard by means of the susceptibility assessment. The term "susceptibility" is employed here to define the likelihood of occurrence of crater-like depressions and submarine landslides in fluid leakage areas. The proposed method, susceptibility assessment, is applied as a first step in the risk assessment: preferably on regional scales and when few historical or temporal records of the activity of the seafloor features are available. We have selected the bivariate statistical index (*Wi*) method proposed by Van Westen (1997), based on the weighting of each class of the map of factors as a function of the density of the seafloor features (submarine landslides or crater-like depressions). This density is measured by means of the *Wi* index as the ratio between the area affected by the seafloor features over the classes of the maps of factors, and the proportion of the total of seafloor features in the study area (see Eq. 1). The proposed statistical index method was developed under a GIS environment. The presented methodology does not establish a priori assumptions or causalities between factors and seafloor features. Only after the statistical analysis and the calculation of the *Wi* index do we establish the link between factors and features and the degree of correlation among them.

Weight calculus

In this method, a weight value for a parameter class is defined as the natural logarithm of the density of seafloor features related to seabed fluid flow in each class, divided by the density of the same seafloor features in the entire map (study area). Weight is the value assigned to each class of a "factor map" according to the number ("density") of seafloor features related to seabed fluid flow identified (in our case, crater-like depressions and submarine landslides). Weights are calculated by comparing the area affected by crater-like depressions or submarine landslides in each class of the factor map with the total study area (Van Westen 1997):

$$Wi = \mathrm{Ln}\left[\frac{Density\ Class}{Density\ Map}\right] = \mathrm{Ln}\left[\frac{Area(Si)/Area(Ni)}{\sum Area(Si)/\sum Area(Ni)}\right] \quad (1)$$

where *Wi* is the weight assigned to a class, *Area*(*Si*) is the area affected by crater-like depressions or submarine landslides in a class, and *Area*(*Ni*) is the total area of a class on the factor map.

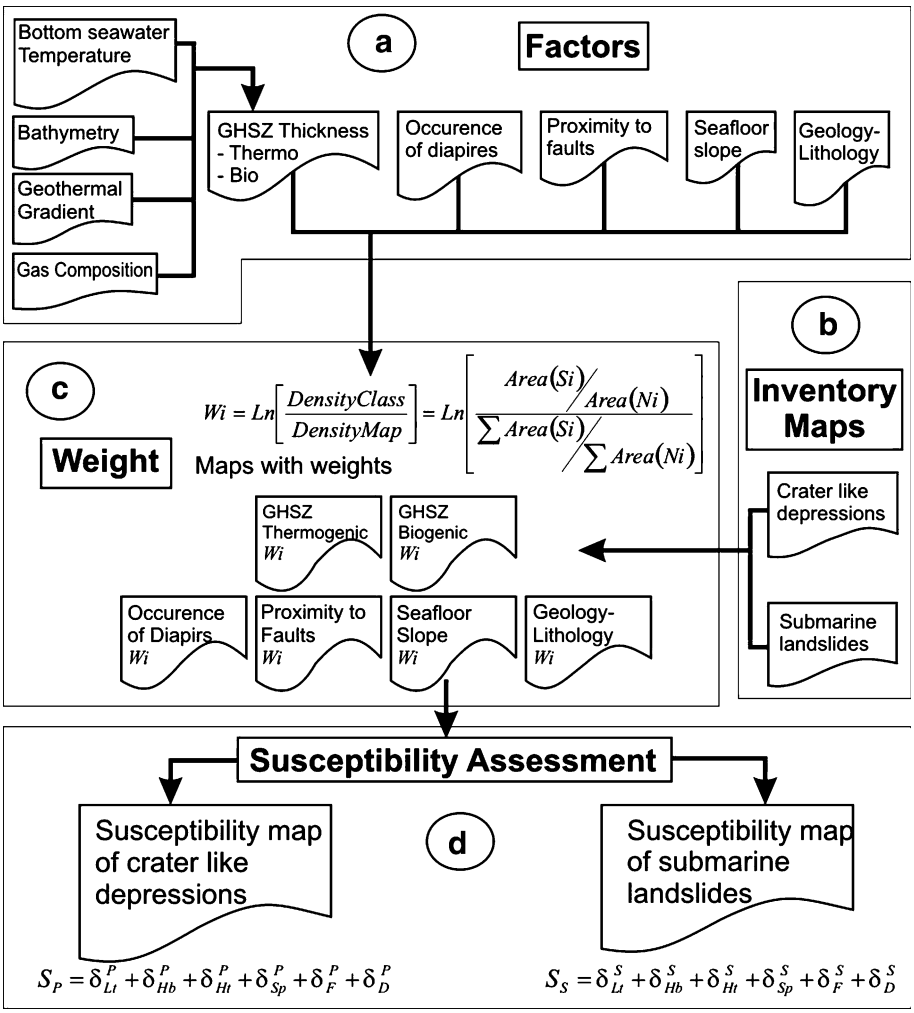

Fig. 3 Flow diagram of work processes for the calculation of susceptibility in the proposed marine model. **a** Analysis of intrinsic and derived factors that might play a role in the generation of seafloor features related to seabed fluid flow. **b** Preparation of the inventory maps, mapping of seafloor crater-like depressions and submarine landslides from MBES data, high-resolution shallow seismic and a VHR Chirp. **c** Weight calculation of every class of factor maps as a function of the density of seafloor features. **d** Susceptibility assessment

The *Wi* method is based on statistical correlation of each inventory map with the attributes of each factor map. In this study, each factor map was crossed with the inventory maps, and the density of seafloor features in each class was calculated. Correlation results were stored in resultant rasters (maps of weights) and the density of seafloor features per parameter class was calculated. Then the *Wi* value of each attribute was calculated (Figs. 3, 7; Table 1). A high *Wi* value means a high correlation, or dependence, between the class and the seafloor feature, so there are many features inside this class. A positive *Wi* value means that the density of seafloor features in the class is higher than the density of seafloor features in the study area. A negative *Wi* value means that the density of seafloor features in the class is lower than the density of seafloor features in the study area.

Susceptibility assessment is analyzed separately, following four steps (Fig. 3): (1) mapping of seafloor crater-like depressions and submarine landslides from MBES data, high-resolution shallow seismic (Sparker) profiles and very high resolution (VHR) chirp data (topographic parametric sonar, TOPAS), and preparation of an inventory map; (2) analysis of intrinsic and derived factors that might play a role in the generation of the seafloor features in a gas-venting area; (3) weight calculation of every class of factor maps as a function of the density of seafloor features; and (4) susceptibility assessment.

Results

Inventory maps of seafloor features related to seabed fluid flow

VHR chirp (TOPAS), Sparker, and MBES data were used for seafloor geomorphic characterization and mapping. Multichannel seismic lines were used for characterization and correlation of seafloor structures to seabed fluid flow, especially in the case of fault systems and seismic chimneys that act as fluid pathways linking buried diapirs to the seafloor (Fernández-Puga et al. 2007; Medialdea et al. 2009, León et al. 2010).

Table 1 Parameters taken into account and values of the *Wi* resulting from the weight calculation of each class of the maps of factor

Study area		Total area	Area with crater like depressions	Area with submarine landslides		
		17141318483	505360114.2		169219544.4	
Factor	Class	Area of the class	Area with crater like depressions	Area with submarine landslides	Weight: "*Wi*" value	
					Crater like depressions	Submarine landslides
GHSZ biogenic	No hydrate	7377455766	151067281.4	67815451.15	−0.36448296	−0.071343886
	GHSZ thinned	5998967570	338242944.1	98961094.33	0.648397586	0.513434287
	GHSZ	3764978535	11984746.93	2026413.328	−2.225886846	−2.90917988
GHSZ thermogenic	No hydrate	11928798111	2850665.664	0	−4.815182391	inf
	GHSZ thinned	1290886611	484856925.6	166762399.1	2.544745133	2.571535646
	GHSZ	3921633799	13597464.09	2026413.328	−2.140404479	−2.949946072
Buried diapirs	Outside	15461733283	270361884.3	127898716.3	−0.522386215	−0.176834595
	Inside	1679585200	230901152.1	40827024.48	1.53966341	0.901092252
Lineaments	Outside	14806336849	219337593.8	88726352.22	−0.688222626	−0.499203432
	Inside	2334981637	282025795.1	80064638.08	1.410215079	1.245125141
Slopes	0–1	10832135082	361926645.9	68872364.03	0.125144936	−0.439967293
	1–2	5097749133	130507512.3	71709465.49	−0.141147738	0.354118557
	2–3	1001800069	8639835.679	8333849.236	−1.22919432	−0.171178109
	3–4	215799531	127550.6467	3329800.104	−3.909615798	0.446612572
	4–5	68070280	0	12044530.2	inf	2.886120115
	5–6	28028939	0	3427868.915	inf	2.516751424
	6–7	4004134	0	0	inf	inf
	>7	12012402	0	1107015.506	inf	2.233778239
Geology lithology	Basement	99778710.02	0	5927695.247	inf	1.794730822
	CDS	13738822653	487960150.8	154002854.4	0.186228716	0.127040441
	Diapir	318686314.7	11992450.26	7375117.169	0.244045873	0.851954688
	Lower slope	2984030568	1292919.203	1726817.891	−4.220151749	−2.836699681

Upper part shows the global parameters of the study area: total area (value to change instead of $\sum Area(Ni)$in Eq. 1); area with crater-like depressions (instead of $\sum Area(Si)$ in Eq. 1 in the crater-like depressions analysis); and area with submarine landslides (instead of $\sum Area(Si)$ in Eq. 1 in the submarine landslide analysis)

Lower part shows the parameters of each class of the map of factor: area of the class (value to change instead of $Area(Ni)$in Eq. 1); area with crater-like depressions (instead of $Area(Ni)$ in Eq. 1 in the crater-like depression analysis); area with submarine landslides (instead of $Area(Ni)$ in Eq. 1 in the submarine landslide analysis). Values in m^2

The inventory map of submarine landslides (Fig. 4a) was generated by including typologies of gravitational instabilities such as slides and slumps (Mulder and Cochonat 1996; Lee et al. 2002). On this map, we identified "zones of seafloor affected by instability processes" as polygons bounded between the submarine landslide scars and the transported deposits, which implies that both erosive and depositional processes affect these areas. All identified features related to gravitational instabilities, whether buried or not, were mapped without taking into account the time span between successive events. Thus, the return period for such features was not calculated.

Submarine landslides are common around the CDS, near the western base of the slope of the Guadalquivir and Cadiz Diapiric Ridges. This area has a smooth slope (0.2°–1.5°) and is formed by a sequence of silty sands and sandy silts (Habgood et al. 2003; Hernández-Molina et al. 2003). Submarine landslides occurring on the slopes (3°–15°) of crater-like depressions, from 530 to 1020 m water depth, range from 1.5 to 4 km in length and from 400 m to 1 km in width. Generally, landslide surfaces are composed of a hummocky relief, the sediment thickness of the deposit is around 70 m, and the slip plane is smooth (<1°) and sub-parallel to the seafloor. Internally patches of transparent acoustic facies with irregular blocks bounded by listric faults are observed (Fig. 8 of León et al. 2009), all of them representing echo type IV-1 of Lee et al. (2002). In this area, submarine landslides are translational, with lobate scars and retrogressive headwalls. In initial stages or on headwalls, rotational blocks can be observed (Fig. 4e).

Outside the CDS, the submarine landslides take place on the steep (10°–20°) slopes of the Guadalquivir Bank, where they are different from those in the rest of the study area. They are discontinuous allochthonous masses of 30 m maximum thickness with transparent seismic facies below a continuous, high-amplitude reflector (Fig. 4b, d). Swath bathymetry shows retrogressive scars and a hummocky relief over the mobilized sediment. In seismic profiles, they show on the seafloor a continuous reflection of high amplitude over transparent acoustic facies (Fig. 4d), with locally hyperbolic reflexions (Fig. 8 of León et al. 2009).

The inventory map of crater-like depressions (Fig. 5a) includes all negative relief related to fluid flow, such as pockmarks and seabed collapses. These features were previously outlined on MBES maps and then correlated with sub-seafloor acoustic anomalies observed in seismic data (Fig. 5b). All the features identified were mapped regardless of their age or degree of activity. Crater-like depressions occur throughout the study area from 850 to 1,450 m water depth. From around 800 m water depth (approximately the upper limit of the theoretical gas hydrate stability zone [GHSZ] for gases of biogenic origin), pockmarks tend to be regularly spaced, smaller-sized, and more homogeneous in size. They are typically cone-shaped (slopes of 15°–25°) and sizes vary widely, from 150 to 950 m in diameter and from 20 to 60 m in depth. Shapes vary from isolated, sub-circular forms to complex forms. Collapses are U-shaped depressions delimited by normal faults with chaotic and blanking acoustic facies. They vary from 500 m to 5 km in diameter and from 20 to 248 m in depth. Shapes range from sub-circular forms to elongated complex forms. Collapses are connected to diapiric structures via focused seismic chimneys. Locally, huge, elongated (ca. 10 km long) collapsed depressions (dead-end valleys) related to other fluid-flow structures such as pockmarks, carbonate-mud mounds and mud volcanoes have been mapped. (León et al. 2010).

Controlling factors of seafloor features related to seabed fluid flow

The factors chosen determine the susceptibility of an area to be disrupted by crater-like depressions and/or submarine landslides caused by seabed fluid flow in the Gulf of Cadiz. We selected geological features or properties that determine the capability of the seabed to store and transfer fluids to the seafloor. The factors were analyzed within two categories: intrinsic and derived factors. Intrinsic factors are measured properties of seafloor sediment or features directly interpreted from data, such as geology-lithology, occurrence of buried salt/shale diapirs, proximity to faults, and slope angle of the seafloor. Derived factors are theoretical features (calculations) deduced from a numerical model with measured properties. To group the derived factors we used the theoretical thickness of the GHSZ beneath the seafloor because it results from the analysis of other factors such as water temperature and pressure (depth) and the rate of temperature rise with depth within the seabed sediments (geothermal gradient).

Geology-lithology

Fluid dynamics and storage typology inside the sediment are controlled by geology and lithology, and depend on sedimentary and tectonic structures, unconformities, granulometry, permeability, porosity, and thickness of the deposit. The map of factor "geology-lithology" contains four classes (Fig. 6a): basement, CDS, outcropped salt/shale diapirs, and lower slope.

Occurrence of buried diapirs

Buried diapirs are areas of potential accumulation of shallow gas, and usually build traps for hydrocarbon fluids

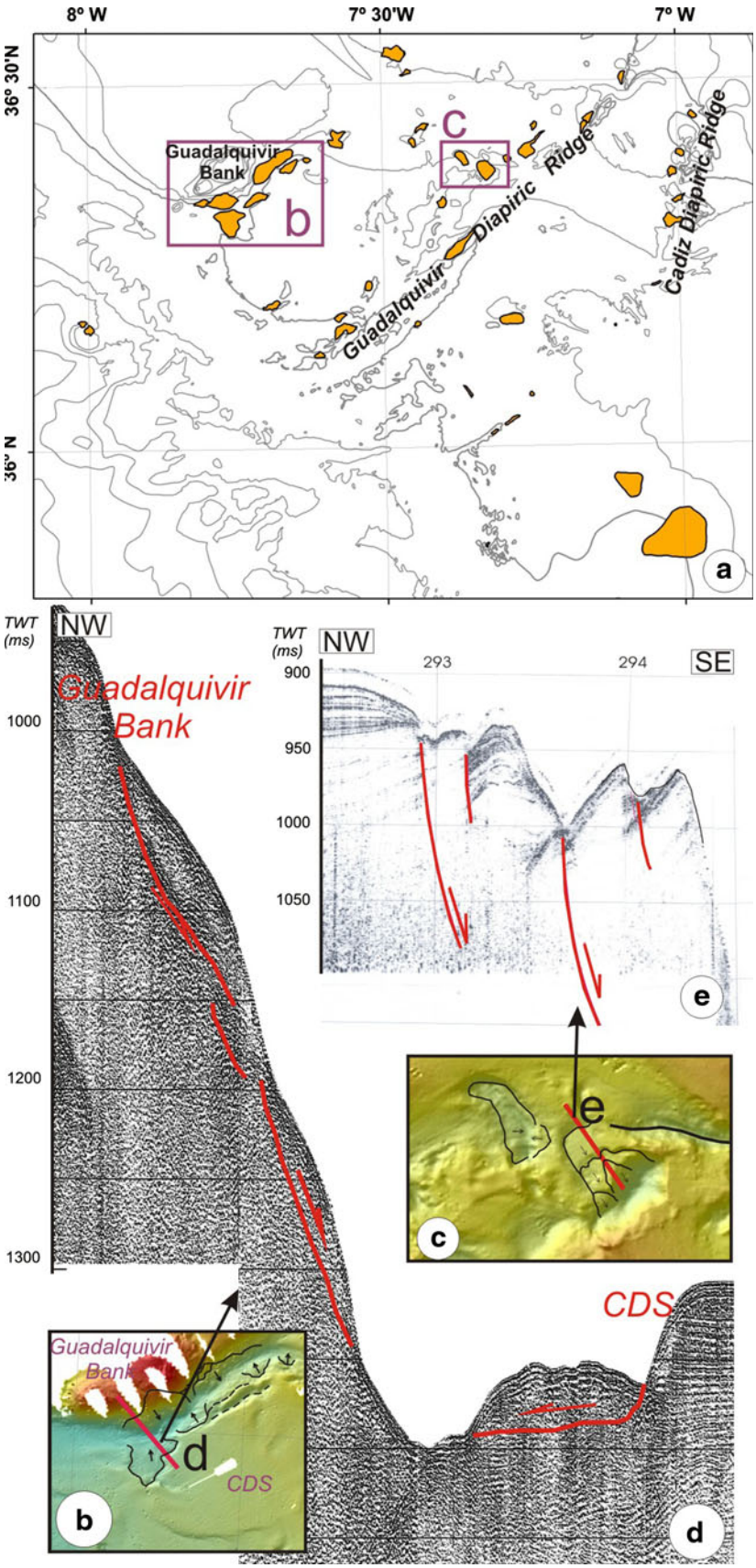

Fig. 4 **a** Inventory map of submarine landslides. **b** Detail of the Guadalquivir Bank. **c** Detail of the Guadalquivir Diapiric Ridge. **d** Sparker seismic profile, *Line 1* of the Anastasya-00 cruise, showing the different typology of submarine landslides between the Guadalquivir Bank and the CDS. **e** TOPAS seismic profile, *Line 22* of the Tasyo 2000 cruise, showing retrogressive rotational blocks on the headwall of a submarine landslide developed in the flank of a crater-like depression of the CDS

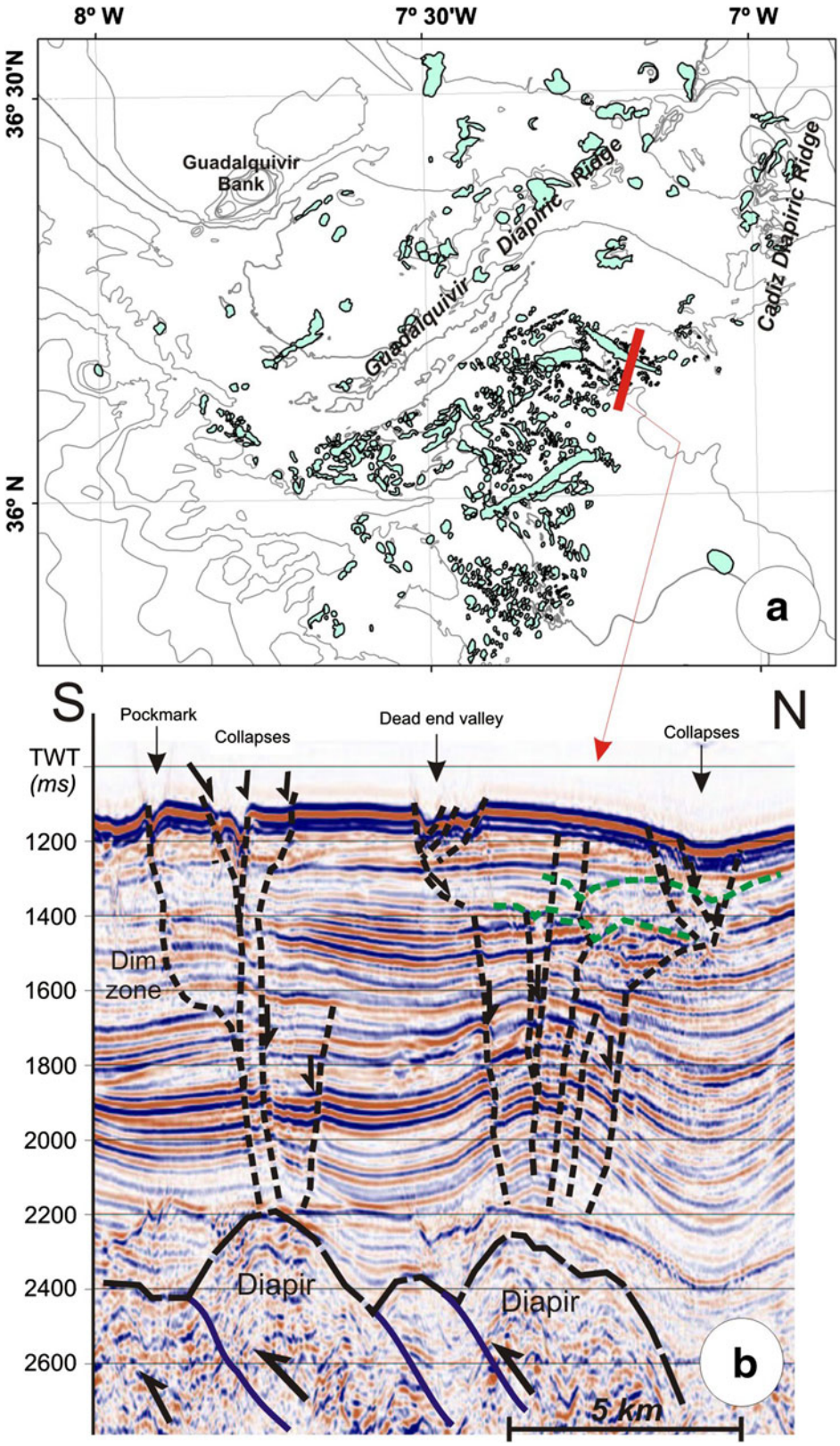

Fig. 5 **a** Inventory map of crater-like depressions. **b** Multichannel seismic profile of the Tasyo 2000 cruise, showing the link between crater-like depressions and diapirs. The different typologies of crater-like depressions (pockmarks, collapses and dead-end valleys) and seismic evidence of fluid flow can be observed in the seismic profile, modified from Léon et al. (2010)

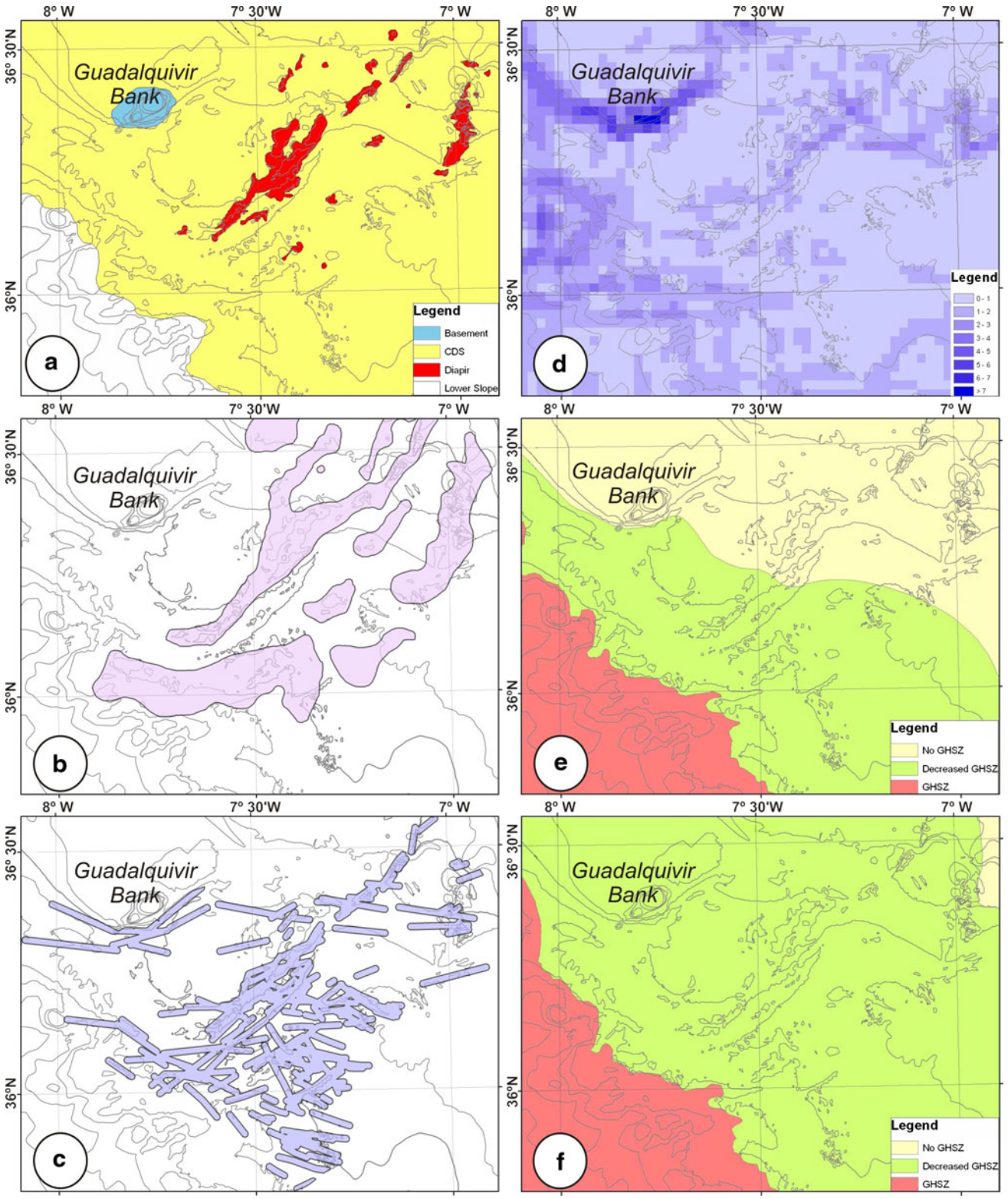

Fig. 6 Factors taken into account in the susceptibility assessment. **a** Geology-lithology map. **b** Occurrence of diapirs, simplified from Fernández-Puga (2004), diapirs in colour. **c** Proximity to faults or lineaments, influence area of faults in colour. **d** Slopes. **e** Theoretical thickness of hydrate stability field from biogenic gases. **f** Theoretical thickness of hydrate stability field from thermogenic gases

expelled from the AUGC. Medium- and deep-penetration seismic profiles indicate methane-related seafloor morphological features that are closely associated with deeper diapiric structures. Fernández-Puga (2004) mapped approximately 20 elongated diapiric structures (Fig. 6b) (4–86 km long) throughout the middle continental slope of the Gulf of Cádiz at water depths of 300 to 1,100 m. Diapirs are related to extensional tectonics (listric fault movement) or compressional tectonics (thrusts). The uplift process deforms the Pliocene-Quaternary sedimentary units and the middle continental slope seafloor. Over buried diapirs, we can observe a great variety of seafloor features related to methane expulsion, such as mud volcanoes, crater-like depressions, submarine landslides, and carbonate mounds. Under these seafloor features and at the top of all types of buried diapirs and dome structures, chaotic and transparent seismic facies and other acoustic anomalies suggest that gas-bearing sediments and upward gas migration through fault structures are related to diapir evolution (Fig. 5b). The map of factor "occurrence of buried diapirs" contains only two classes (Fig. 6b): presence or absence (no diapirs).

Proximity to faults or lineaments

A map of linear features was constructed based on the MBES data. When these seafloor linear features were also identified on seismic profiles they were labelled as "faults", and otherwise as "lineaments". The map of factor "proximity to fault or lineament" is a polygonal map built around each fault and lineament with a specified distance of influence. We selected 1500 m for the distance of influence because this is the mean value size of the geological structures related to fluid flow identified in the Gulf of Cádiz. Finally, we selected only two classes in the map of factor "proximity to fault or lineament": inside and outside the area of influence (Fig. 6c).

Slope angle of the seafloor

Slope angle is very frequently used in landslide susceptibility studies. It is a factor describing geometrical predisposition to gravitational instabilities of the pile of sediments. Submarine landslides mostly occur at a certain critical slope angle. Once the lateral component of the weight of sediment overcomes its internal friction and cohesion, sediment tends to move down-slope (Ayala et al. 1987). The slope map of the seafloor (Fig. 6d) represents areas of equal inclination and stores the value, in degrees, between the seafloor and horizontal. The factor map of slope was segmented into six classes, the interval of each class being 1 degree. This 1° interval was used in other statistical works in the eastern North Atlantic (Hühnerbach and Masson 2004).

Theoretical thickness of the hydrate stability field

We established the theoretical thickness of the hydrate stability field as a factor due to the direct and indirect evidences of hydrates in the Gulf of Cadiz. We used the theoretical thickness of the hydrate stability field calculated by León et al. (2009) from both biogenic and thermogenic gases. We divided the map of factor "GHSZ thickness" into three categories (Figs. 6e, f), the first two being: (1) seafloor outside the hydrate stability field and (2) seafloor inside the hydrate stability field. However, the occurrence of warm water masses flowing episodically over the seafloor (as in the case of the Gulf of Cadiz) requires an additional category to be introduced on the map: (3) seafloor inside the hydrate stability field with reduced GHSZ due to warming of the MOW undercurrent.

Maps of susceptibility assessment

The final susceptibility maps were obtained by adding all weighted layers (Figs. 7, 8). Each pixel value of the final susceptibility map is the algebraic addition of pixel values (with the same geographic location) of each map of weights. The final susceptibility maps were segmented into five equal intervals according to the total number of elements: very low susceptibility, low susceptibility, moderate susceptibility, high susceptibility, and very high susceptibility.

Seafloor susceptibility to crater-like depressions (S_P) (Fig. 8a) is the sum of six maps of weights for crater-like depressions corresponding to: map of geology-lithology (δ^P_{Lt}) + map of hydrate thickness (biogenic origin) (δ^P_{Hb}) + map of hydrate thickness (thermogenic origin) (δ^P_{Ht}) + map of slope angle of the seafloor (δ^P_{Sp}) + map of lineaments and faults (δ^P_F) + map of diapirs (δ^P_D):

$$S_P = \delta^P_{Lt} + \delta^P_{Hb} + \delta^P_{Ht} + \delta^P_{Sp} + \delta^P_F + \delta^P_D \quad (2)$$

Values in the map of crater-like depression susceptibility are high inside the theoretical hydrate stability field reduced by warming of the MOW undercurrent, in zones with contourite deposits over buried diapirs, and close to faults or lineaments. Therefore, the areas particularly predisposed to generating pockmarks occur in fine-grained sediments, such as the CDS, over buried gas-storing structures (diapirs) connected to pathways of fluid escape (faults) and affected by the MOW undercurrent (the reduced theoretical GHSZ thickness). The Palaeozoic basement shows a very low susceptibility.

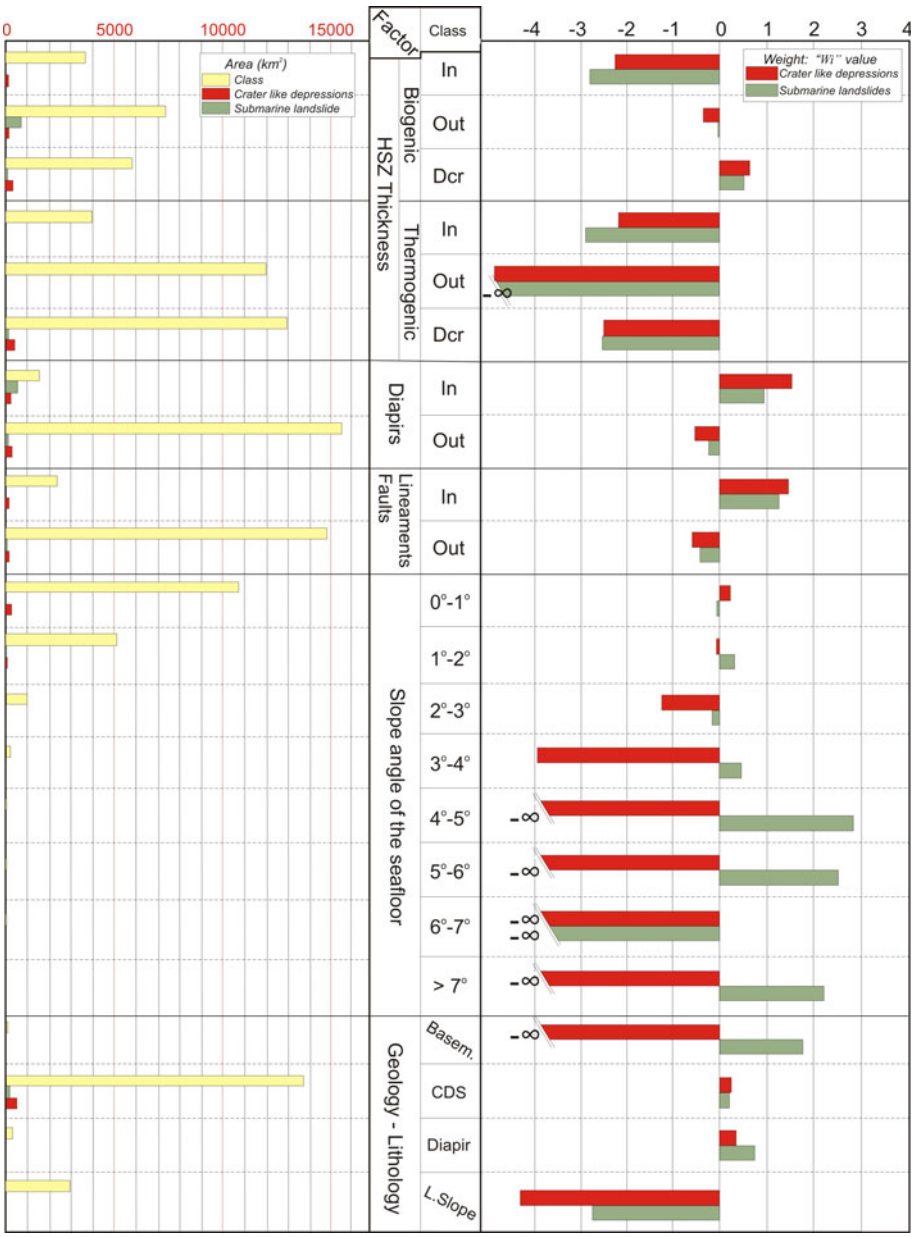

Fig. 7 Chart showing the results of the weight calculation of each class of the factor maps. *Right side* shows the weights of the maps of factors calculated from the density of submarine landslides and crater-like depressions (collapses and pockmarks) within individual classes. *Left side* represents the area of each class versus the area of crater-like depressions and submarine landslides. For GHSZ thickness factor: *In* inside; *Out* outside; *Dcr* decreased thickness of the GHSZ

Similarly, the seafloor susceptibility to submarine landslides (S_S) (Fig. 8b) is the sum of the following six maps of weights for submarine landslides:

$$S_s = \delta^S_{Lt} + \delta^S_{Hb} + \delta^S_{Ht} + \delta^S_{Sp} + \delta^S_F + \delta^S_D \quad (3)$$

Where: δ^S_{Lt}, map of geology-lithology weighted to submarine landslides; δ^S_{Hb}, map of hydrate thickness (biogenic origin) weighted to submarine landslides; δ^S_{Ht}, map of hydrate thickness (thermogenic origin) weighted to submarine landslides; δ^S_{Sp}, map of the slope angle of the seafloor weighted to submarine landslides; δ^S_F, map of lineaments and faults weighted to submarine landslides; δ^S_D, map of diapirs weighted to submarine landslides

Submarine landslide susceptibility maps show two different geologic areas where susceptibility is moderate to high. The first is located over the steep slopes of the Guadalquivir Bank. In this area, susceptibility seems to be related only to the factor of slope angle and geology-lithology, and not to the other factors associated with fluid flow. The second area is located over the smooth relief of the CDS on the western side of the base of the slope of the Guadalquivir and Cadiz Diapiric Ridges, where submarine landslides are related to crater-like depressions. Susceptibility seems to be controlled by buried diapirs, proximity to lineaments, and the theoretical GHSZ thickness reduced by the MOW.

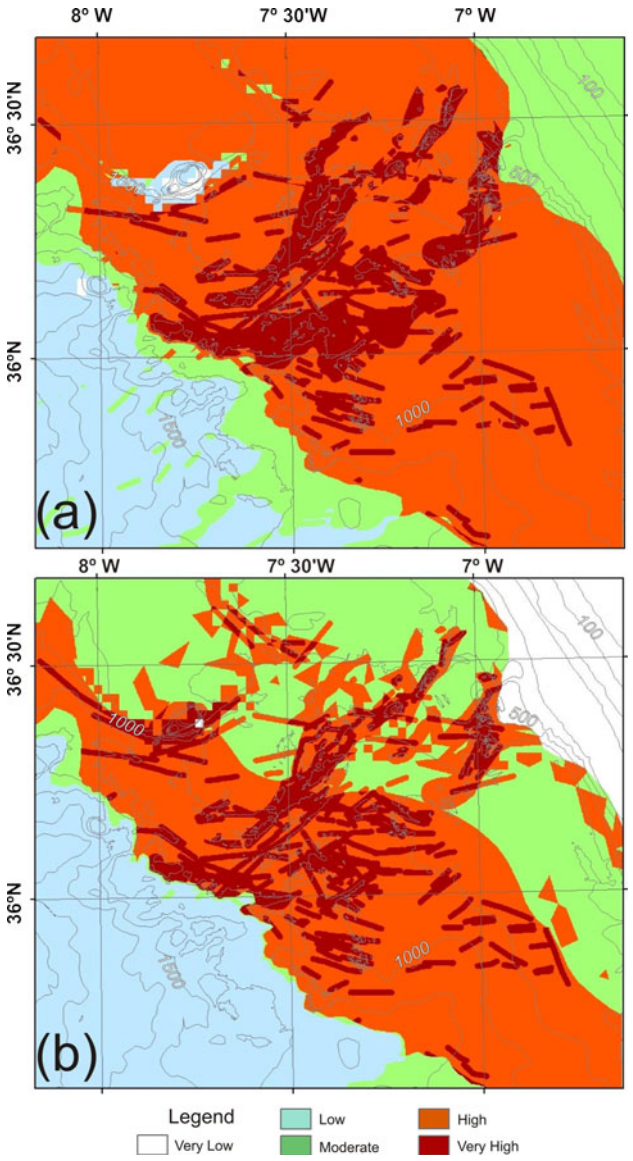

Fig. 8 Seafloor susceptibility maps. **a** Susceptibility to crater-like depressions. **b** Susceptibility to submarine landslides), segmented by quantiles in five categories: very high, high, medium, low, and very low

Discussion

Comparison of marine vs terrestrial GIS-based bivariate mapping

In this paper we present the application to marine environments of the methodology tested on land at scales ranging from 1:25,000 to 1:50,000 (Varnes 1984; Soeters and van Westen 1996; Çevik and Topal 2003). However, the difference of quantity/density and accuracy of data between marine and terrestrial environments requires different work scales for the two environments. The density and accuracy of data in the present paper is suitable for mapping at scales between 1:100,000 and 1:200,000, which are used in regional studies as a first step or a baseline in the process of risk assessment. These differences in quantity/density, accuracy, and work scale could be the reason for the different number of variables (map of factors) involved in the susceptibility analysis in the two environments.

Advantages of the proposed method are its easy application and the fact that it can be used to calibrate in situ quantitative data or to obtain results at regional scales by extrapolating these data. Another advantage is the possibility of obtaining a numeric value to assess the correlation or dependence of one factor in the generation of a seafloor feature. However, the proposed method has some constraints or limitations. The first is that it is essential to have a reliable understanding of the geologic model of the study area because the selection of factors and assumptions is based on expert criteria. The expert criteria introduce a degree of subjectivity, giving the results an uncertainty that is difficult to measure.

Other interpretations of the seafloor features and error assessment of the methodology

The MOW bottom current flowing through single, crater-like depressions may be enlarged by erosion and linked to others, giving rise to elongated features. The assessment of susceptibility to these "modified" crater-like depressions is thus subject to a degree of uncertainty because the size of the depressions is the result of at least two geological processes: intermittent gas bursts (eruptions) and extended intervening periods of slow, diffusive pore-water seepage (Hovland et al. 2010), during which the predominant process is erosion by bottom undercurrents. The areal density distribution of the crater-like depressions thus induces a small degree of uncertainty when they are related to the intensity of gas-seep activity.

Crater-like depressions and submarine landslides have an irregular surface and locally are masked or partially masked by sediment waves (Leon et al. 2010). For this reason, many of these seafloor features have been interpreted as erosive features, sediment forms, or wave fields (Kenyon and Belderson 1973; Habgood et al. 2003; García et al. 2009). Swath bathymetry, VHR Chirp, and multichannel seismic profiles have given more precise seafloor images and revealed new properties of seafloor morphology, showing that crater-like depressions and submarine landslides have a link with the fluid flow coming from diapirs.

It is very difficult to obtain a numeric value of the error or uncertainty of the present approach. In our opinion, this is beyond the scope of this paper. The calculation of error

would take into account the error made in the definition of each variable and factor. This is possible in the calculation of the oceanographic variables (León et al. 2009). However, the great problem is to assess the error in the mapping of seafloor features, which are interpreted with a high degree of subjectivity by researchers. Furthermore, when we take data from publications (e.g. Fernández-Puga 2004), it is impossible to perform an error assessment as we do not know how these data were built. Nevertheless, we can obtain an idea of the sensitivity of the estimation of the presented method from the *Wi* index. The estimation will be more sensitive to the spatial location of factors with a high *Wi* and the uncertainty of hypotheses deduced from the factors with a high *Wi* value will be low.

Submarine landslides: triggers and role of the slope angle of the seafloor

Throughout the study area, only where the basement is outcropping (the Guadalquivir Bank) do the submarine landslides show high sensitivity to the slope angle of the seafloor factor. This fact indicates that the slope angle of the seafloor and earthquakes is the main trigger, as suggested by Mulder et al. (2009). This contradicts Canals et al. (2004) and Hühnerbach and Masson (2004), but the submarine landslides in the Guadalquivir Bank are very different in lithology (basement) and size (20,000 times smaller) than those mentioned by their studies.

The submarine landslides in the CDS area are different and involve mainly contourite deposits where diapirism and fluid seepage take place. In this area, other trigger mechanisms are suggested, such as: (1) high sedimentation rates leading to excess pore pressure (overpressurized layers) and underconsolidation (weak layers); (2) fluid seepage and bubble-phase gas charging; (3) diapirism and faulting; (4) incision of the MOW undercurrent; and (5) dissociation of gas hydrates.

The CDS thickness of up to 600 m and rates of accumulation of 14.5 cm ky^{-1} (Stow et al. 2002) will tend to increase the excess pore pressure. In turn, the effective strength of sediments barely increases with sediment burial, thus being lower than expected. The clayey units of the contourite units that were deposited during interglacials and transitions play a role in the development of mechanical discontinuities and weak layers, having great potential to behave as slip planes. Furthermore, fluid venting indicates overpressure and that the area could be prone to failure. Therefore, in the CDS we could postulate that slope and potential slip-plane angles are not the main requirement for submarine landslide events. In fact, submarine landslides occur on slopes of less than 16°, the static condition defined by Lee and Baraza (1999). On the basis of our statistical analysis, the only reason for justifying the different main requirements for submarine landslide events between the CDS and the Guadalquivir Bank lies in the lithology-geology factor and the great difference in the cohesion of the sediments.

Dependence of seafloor features and factors: role of fluid flow

Wi values show a clear dependence on buried diapirs, faults, and theoretical GHSZ thickness. The majority of pockmarks and collapses occur in the theoretical GHSZ thickness reduced by the MOW, associated with buried diapirs (not in outcropped diapirs), over the CDS, and near faults. Most of them are covered by HDACs (Díaz-del-Río et al. 2003), clearly indicating a relationship of the fluid flow from diapirs through fine-grained sediments. The high susceptibility to crater-like depressions matches with the factors "occurrence of diapirs" and "proximity to fault or lineaments", in agreement with the previous geological models proposed in the Gulf of Cadiz (Fernández-Puga et al. 2007; Medialdea et al. 2009; León et al. 2010).

Gas hydrates and their dissociation have often been associated with slope instability (Hampton et al. 1996). Natural gas and hydrates have been identified in the Gulf of Cádiz (Ivanov et al. 2000; Mazurenko et al. 2003) but hydrates have only been recovered over mud volcanoes with both a disperse (e.g. Ginsburg mud volcano; Ivanov et al. 2000) and a laminar texture (e.g. Bojardim mud volcano; Mazurenko et al. 2003; Kopf et al. 2004). Furthermore, no hydrates have been detected in any other geological features such as pockmarks or collapses. The lack of gas or hydrate evidence on crater-like depressions could also be related to a problem of density of data (few samples). HDACs recovered in crater-like depressions show an isotopic composition (depletion in $\delta^{13}C$ and enrichment in $\delta^{18}O$) compatible with possible undated massive gas hydrate dissociation (Díaz-del-Río et al. 2003). However, the dependence between seafloor features and reduced GHSZ thickness for biogenic gases (the only class with positive *Wi* values in this factor map) point to a possible former relationship between seafloor features and hydrate dissociation.

Global sea-level changes and the subsequent episodic warming by the MOW undercurrents could be considered the most plausible scenarios for a massive hydrate dissociation in the Gulf of Cádiz (León et al. 2010). Potential consequences of these dissociations would be: (a) a release of water and gas, (b) a rapid reduction in sediment strength, and (c) an increase in pore fluid pressure. All these consequences may act as triggering factors for the development of crater-like depressions and submarine landslides in these areas. Thus, changes in seawater temperature due to the "periodic" influence of different ocean bottom waters,

as in the Gulf of Mexico and the South American Atlantic margin (MacDonald et al. 1994), may produce natural dissociation of gas hydrates exposed on the seabed.

Conclusions

In the Gulf of Cadiz we have successfully applied a GIS-based method for assessing seafloor failure susceptibility in fluid leakage areas. The method has been previously used onshore, but in this study it was used for the first time for offshore deepwater. The susceptibility assessment defines the likelihood of occurrence of a geological process such as seabed collapse, fluid escape, and submarine landslides. The proposed method is an advantageous tool for mapping geohazards in regional studies as a first approach in geological risk assessment.

The factors used to determine the susceptibility to marine geohazards in a fluid leakage area can be grouped into two categories: (1) intrinsic factors, which are measured properties of the sediment or features directly interpreted from data that have played a role in the generation of the seafloor features related to seabed fluid flow (geology-lithology, occurrence of buried salt/shale diapirs, proximity to faults, and slope angle of the seafloor); and (2) derived factors, which are theoretical features deduced from a numerical model with measured properties (theoretical thickness of the GHSZ).

Susceptibility to crater-like depressions is high inside the theoretical GHSZ reduced by warming of the MOW undercurrent, in contourite sediments over salt/shale domes or buried diapiric ridges, and in the vicinity of faults or lineaments. Therefore, the areas particularly predisposed to generating pockmarks appear in fine-grained sediments affected by the warm MOW undercurrent (CDS), over buried gas-storing structures (diapirs) connected to pathways of fluid escape (faults).

Submarine landslide susceptibility maps show two different geologic areas where susceptibility is moderate to high. The first is located on the steep slopes of the Guadalquivir Bank, where susceptibility seems to be controlled by the angle of the slope and is probably not related to fluid flow. The second is located on the smooth relief of the CDS on the western side of the base of the slope of the Guadalquivir and Cadiz Diapiric Ridges. Here, submarine landslide susceptibility is correlated with the same factors as crater-like depressions, and a slope angle of the seafloor is not the main requirement for submarine landslide events to occur.

Acknowledgments We are grateful to all participants in the Tasyo and Anastasya research cruises: the captains, technicians and crews of R/V *Cornide de Saavedra* and R/V *Hespérides*. Special thanks are due to the projects Cadisar (UMR CNRS 5805, France), Gap (Germany) and Golfo (SMAR99-0643T, Spain) for contributing oceanographic data to this study. We are especially grateful to Michael Ivanov and Luis Pinheiro for their helpful co-operation within the framework of the TTR IOC/UNESCO Programme. Thanks are extended to REPSOL-YPF for their helpful collaboration. This work is currently supported by the Spanish Department for Research and Innovation (MICINN) projects CONTOURIBER (CTM 2008-06399-C04/MAR and GLOBANT (CTM 2008-06386-C02/ANT). It is also a contribution to the European Action COST ES0902 "Permafrost and gas hydrate related methane release in the Arctic and impact on climate change: European cooperation for long-term monitoring (PERGAMON)".

References

Ayala FJ, Elízaga E, González de Vallejo LI (1987) Impacto económico y social de los riesgos geológicos en España. Serie geología ambiental. Riesgos Geológicos. I.G.M.E. 91 pp

Baldy P, Boillot G, Dupeuble PA, Malod J, Moita I, Mougenot D (1977) Carte géologique du plateau continental sud-portugais et sud-espagnol (Golfe de Cadiz). Bulletin de la Société Géologique de France 19(7):703–724

Baraza J, Ercilla G (1996) Gas-charged sediments and large pockmark like features on the Gulf of Cadiz slope (SW Spain). Mar Pet Geol 13:253–261

Bayon G, Pierre C, Etoubleau J, Voisset M, Cauquil E, Marsset T, Sultan N, Le Drezen E, Fouquet Y (2007) Sr/Ca and Mg/Ca ratios in Niger delta sediments: implications for authigenic carbonate genesis in cold seep environments. Mar Geol 241(1/4): 93–109

Bower A, Serra N, Ambar I (2002) Structure of the Mediterranean undercurrent and Mediterranean water spreading around the southwestern Iberian Peninsula. J Geophys Res 107(C10):3161. doi:10.1029/2001JC001007

Canals M, Lastras G, Urgeles R, Casamor JL, Mienert J, Cattaneo A, De Batist M, Haflidason H, Imbo Y, Laberg JS, Locat J, Long D, Longva O, Masson DG, Sultan N, Trincardi F, Bryn P (2004) Slope failure dynamics and impacts from seafloor and shallow sub-seafloor geophysical data: case studies from the COSTA project. Mar Geol 213:9–72

Carrara A, Cardinali M, Detti R, Guzzetti F, Pasqui V, Reichenbach P (1991) GIS techniques and statistical models in evaluating landslide hazard. Earth Surf Proc Landf 16:427–445

Casas D, Ercilla G, Baraza J (2003) Acoustic evidences of gas in the continental slope sediments of the Gulf of Cadiz (E Atlantic). Geo-Mar Lett 23:300–310

Çevik E, Topal T (2003) GIS-based landslide susceptibility mapping for problematic segment of the natural gas pipeline, Hendek, Turkey. Env Geol 44:949–962

Cochonat P, Cadet JP, Lallemant SJ, Mazzoti S, Nouzé H, Fouchet C, Foucher JP (2002) Slope instabilities and gravity processes in fluid migration and tectonically active environment in the eastern Nankai accretionary wedge (KAIKO-Tokai'96 cruise). Mar Geol 187:193–202

Depreiter D, Poort J, Van Reesbergen P, Henriet J (2005) Geophysical evidence of gas hydrates in shallow submarine mud volcanoes on the Moroccan margin. J Geophys Res 110:B10103. doi:10.1029/2005JB003622

Díaz-del-Río V, Somoza L, Martínez-Frías J, Mata P, Delgado A, Hernández-Molina FJ, Lunar R, Martín-Rubí JA, Maestro A, Fernández-Puga MC, León R, Llave E, Medialdea T, Vázquez T, Hernández-Molina FJ (2003) Vast fields of hydrocarbon-derived carbonate chimneys related to the accretionary wedge/olistostrome of the Gulf of Cadiz. Mar Geol 195:177–200

Elverhøi A, De Blasio FV, Butt FA, Issler D, Harbitz CB, Engvik L, Solheim A, Marr J (2002) Submarine mass-wasting on glacially influenced continental slopes—processes and dynamics. In: Dowdeswell JA, O'Cofaigh C (eds) Glacier-influenced Sedimentation on high latitude continental margins. Geol Soc Lond Spec Pub 203:73–87

Evans D, King EL, Kenyon NH, Brett C, Wallis D (1996) Evidence for long-term instability in the Storegga slide region off western Norway. Mar Geol 130:281–292

Faugéres JC, Gonthier E, Stow DAV (1984) Contourite drift molded by deep Mediterranean outflow. Geology 12:296–300

Fernández-Puga MC (2004) Diapirismo y estructuras de expulsión de gases hidrocarburos en el talud continental del Golfo de Cádiz. PhD Thesis, Universidad de Cádiz, 336 pp

Fernández-Puga MC, Vázquez JT, Somoza L, Díaz-del-Río V, Medialdea T, Mata MP, León R (2007) Gas-related morphologies and diapirism in the Gulf of Cádiz. Geo-Mar Lett 27: 213–221

García M, Hernández-Molina FJ, Llave E, Stow DAV, León R, Fernández-Puga MC, Diaz del Río V, Somoza L (2009) Contourite erosive features caused by the Mediterranean outflow water in the Gulf of Cadiz: quaternary tectonic and oceanographic implications. Mar Geol 257(1/4):24–40

Gardner JM (2001) Mud volcanoes revealed and sampled on the western Moroccan continental margin. Geophys Res Lett 28: 339–342

Gay A, Lopez M, Berndt C, Séranne M (2007) Geological controls on focused fluid flow associated with seafloor seeps in the Lower Congo Basin. Mar Geol 244(1/4):68–92

GEBCO (2003) GEBCO, 2003 Centenary edition of the GEBCO digital atlas. Published on CD-ROM on behalf of the Intergovernmental Oceanographic Commission and the International Hydrographic Organization as part of the general bathymetric chart of the oceans. CD ROM 551.462.2 GEB.35 2003

Grevemeyer I, Kaul N, Kopf A (2009) Heat flow anomalies in the Gulf of Cadiz and off Cape San Vincente, Portugal. Mar Pet Geol 26:795–804

Habgood EL, Kenyon NH, Masson DG, Akhmetzhanov A, Weaver PPE, Gardner J, Mulder T (2003) Deep-water sediment wave fields, bottom current sand channels and gravity flow channel-lobe systems: Gulf of Cadiz, NE Atlantic. Sedimentology 50:483–510

Hampton MA, Lee HJ, Locat J (1996) Submarine landslides. Rev Geophys 34(1):33–59

Heggland R (1998) Gas seepage as an indicator of deeper prospective reservoirs. A study based on exploration 3D seismic data. Mar Pet Geol 15:1–9

Hernández-Molina FJ, Llave E, Somoza L, Fernández-Puga MC, Maestro A, León R, Medialdea T, Barnolas A, García M, Díaz-del-Río V, Fernández-Salas LM, Vázquez JT, Lobo FJ, Alveirinho-Dias JA, Rodero J, Gardner J (2003) Looking for clues to paleoceanographic imprints: a diagnosis of the Gulf of Cadiz contourite depositional systems. Geology 31:19–22

Hovland M, Judd A (1988) Seabed pockmarks and seepages. Impact in geology, biology and the marine enviroment. Graham and Trotman, London

Hovland M, Heggland R, de Vries MH, Tjelta TI (2010) Unit-Pockmarks and their potential significance for predicting fluid flow. Mar Petrol Geol. doi:10.1016/j.marpetgeo.2010.02.005

Hühnerbach V, Masson DG (2004) Landslides in the North Atlantic and its adjacent seas: an analysis of their morphology, setting and behaviour. Mar Geol 213:343–362

IGME (2003) Mapa geológico de la plataforma continental española y zonas adyacentes. Memoria y Hoja no. 86-86S (Cádiz). Servicio de Publicaciones del Ministerio de Ciencia y Tecnología. Instituto Geológico y Minero de España. Madrid. Escala 1:200.000

Ivanov MK, Kenyon N, Nielsen T, Wheeler A, Monteiro H, Gradner J, Comas M, Akhmanov A, Akhmetzhanov G (2000) Goals and principal results of the TTR-9 cruise. IOC/UNESCO workshop report 168:3–4

Judd A, Hovland M (2007) Seabed fluid flow: the impact on geology, biology and the marine environment. Cambridge University Press, UK

Kenyon NH, Belderson RH (1973) Bed forms of the Mediterranean undercurrent observed with side-scan sonar. Sediment Geol 9:77–99

Kenyon N, Ivanov MK, Akhmetzhanov A, Akhmanov G (2000) Multidisciplinary study of geological processes on the North East Atlantic and Western Mediterranean Margins. Preliminary results of geological and geophysical investigations during TTR-9 cruise of R/V Professor Logachev Intergovernmental Oceanographic Commission technical Series, vol 56, p 56

Kopf A, Bannert B, Brückmann W, Dorschel B, Foubert ATG, Grevemeyer I, Gutscher MA, Hebbeln D, Heesemann B, Hensen C, Kaul NE, Lutz M, Magalhaes VH, Marquardt MJ, Marti AV, Nass KS, Neubert N, Niemann H, Nuzzo M, Poort JPD, Rosiak UD, Sahling H, Scheneider J, Somoza L, Thiebot E, Wilkop TP (2004) Report and preliminary results of sonne cruise SO175. Miami-Bremerhaven, 12.11-30.12.2003. Berichte aus dem Fachbereich Geowissenschaften der Universität Bremen. 228, 231 pp

Lee H, Baraza J (1999) Geotechnical characteristics and slope stability in the Gulf of Cadiz. Mar Geol 155:173–190

Lee SH, Chough SK, Back GC, Kim YB (2002) Chirp (2–7 kHz) echo character of South Korea plateau East Sea: styles of mass movement and sediment gravity flow. Mar Geol 184:227–247

León R, Somoza L, Medialdea T, Maestro A, Díaz-del-Río V, Fernández-Puga MC (2006) Classification of sea-floor features associated with methane seeps along the Gulf of Cádiz continental margin. Deep-Sea Res II 53:1464–1481

León R, Somoza L, Gimenez-Moreno CJ, Dabrio CJ, Ercilla G, Praeg D, Díaz-del-Río V, Gomez-Delgado M (2009) A predictive numerical model for potential mapping of gas hydrate stability zone in the Gulf of Cadiz. Mar Petrol Geol 26:1564–1579

León R, Somoza L, Medialdea T, Hernández-Molina FJ, Vázquez JT, Díaz-del-Río V, González FJ (2010) Pockmarks, collapses and blind valleys in the Gulf of Cádiz. Geo-Mar Lett. ISSN 0276-0460 (Print) pp 1432–1157 (Online), doi:10.1007/s00367-009-0169-z

MacDonald IR, Guinnaso NL Jr, Sassen R, Brooks JM, Lee L, Scott KT (1994) Gas hydrate that breaches the sea floor on continental slope of the Gulf of Mexico. Geology 22:699–702

Maldonado A, Somoza L, Pallarés L (1999) The Betic orogen and the Iberian-African boundary in the Gulf of Cadiz: geological evolution (central North Atlantic). Mar Geol 155:9–43

Mazurenko LL, Soloviev VA, Gardner JM, Ivanov MK (2003) Gas hydrates in the Ginsburg and Yuma mud volcano sediments (Moroccan margin): results of chemical and isotopic studies of pore water. Mar Geol 195:201–210

Medialdea T, Vegas R, Somoza L, Vázquez JT, Maldonado A, Díaz-del-Río V, Maestro A, Córdoba D, Fernández-Puga MC (2004) Structure and evolution of the "Olistostrome" complex of the Gibraltar Arc in the Gulf of Cadiz (eastern Central Atlantic): evidence from two long seismic cross-sections. Mar Geol 209:173–198

Medialdea T, Somoza L, Pinheiro LM, Fernández-Puga MC, Vázquez JT, León R, Ivanov MK, Magalhaes V, Díaz-del-Río V, Vegas R (2009) Tectonics and mud volcano development in the Gulf of Cádiz. Mar Geol 261:48–63

Mulder T, Cochonat P (1996) Classification of offshore mass movements. J Sediment Res 66:43–57

Mulder T, Gonthier E, Lecroart P, Hanquiez V, Marches E, Voisset M (2009) Sediment failures and flows in the Gulf of Cadiz (eastern Atlantic). Mar Petrol Geol 26:660–672

Ochoa J, Bray NA (1991) Water mass exchange in the Gulf of Cadiz. Deep-Sea Res 38:S465–S503

Pinheiro LM, Ivanov MK, Sautkin A, Akhmanov G, Magalhaes VH, Volkonskaya A, Monteiro JH, Somoza L, Gardner J, Hamouni N, Cunha MR (2003) Mud volcanism in the Gulf of Cadiz: results from the TTR-10 cruise. Mar Geol 195:131–151

Platt JP, Anczkiewicz R, Soto JI, Kelley SP, Thirlwall M (2006) Early miocene continental subduction and rapid exhumation in the western Mediterranean. Geology 34:981–984

Prior DB, Coleman JB (1984) Submarine slope instability. In: Brunsden D, Prior DB (eds) Slope instability. Wiley, New York, pp 419–455

Serviços Geológicos de Portugal (1992) Carta Geológica de Portugal a escala 1:500000. Serviços Geológicos de Portugal

Soeters R, Van Westen CJ (1996) Slope instability recognition, analysis and zonation. In: Turner AK, Schuster RL (eds) Landslides investigation and mitigation: transportation research board special report 247. National Academy Press, Washington, pp 19–177

Somoza L, Hernández-Molina FJ, Vázquez JT, García-García A, Díaz-del-Río V (2000) El nivel de ''BSR'' en el talud superior del Golfo de Cadiz: implicaciones tecto-sedimentarias y paleoceanograficas. Congreso Geológico de España, Alicante

Somoza L, Gardner JM, Díaz-del-Río V, Vázquez JT, Pinheiro LM, Hernández-Molina FJ, TASYO/ANASTASYA Shipboard Scientific Parties (2002) Numerous methane gas-related sea floor structures identified in Gulf of Cadiz. EOS Transactions 83, 47:541–547

Somoza L, Díaz-del-Río V, León R, Ivanov M, Fernández-Puga MC, Gardner JM, Hernández-Molina FJ, Pinheiro LM, Rodero J, Lobato A, Maestro A, Vázquez JT, Medialdea T, Fernández-Salas LM (2003) Seabed morphology and hydrocarbon seepage in the Gulf of Cadiz mud volcano area: acoustic imagery, multibeam and ultra-high resolution seismic data. Sedimentary processes and seafloor hydrocarbon emission on deep European Continental margins. Mar Geol 195:153–176

Stow DAV, Faugères JC, Gonthier E, Cremer M, Llave E, Hernández-Molina FJ, Somoza L, V. Díaz-Del-Río V (2002) Faro-Albufeira drift complex, northern Gulf of Cadiz. Deep-water contourite systems: modern drifts and ancient series, seismic and sedimentary characteristics. Geol Soc, London, Memoirs, 22: 137–154

Sultan N, Cochonat P, Bourillet JF, Cayocca F (2001) Evaluation of the risk of marine slope instability: a pseudo-3D approach for application to large areas. Mar Georesour Geotechnol 19:107–133

Van Westen CJ (1997) Statistical landslide hazard analysis. ILWIS 2.1 for Windows application guide. ITC Publication, Enschede, pp 73–84

Van Westen CJ, Terlien TJ (1996) An approach towards deterministic landslide hazard analysis in GIS. A case study from Manizales (Colombia). Earth Surf Proc Landf 21:853–868

Varnes DJ (1984) Landslide hazard zonation: a review of principles and practice. UNESCO, Paris

Wilson CK, Long D, Bulat J (2003) The Afen slide a multistaged slope failure in the Faeroe-Shetland channel. In: Locat J, Mienert J (eds) Submarine mass movements and their consequences. Kluwer Academic Publishers, Dordrecht, pp 317–324

Yun JW, Orange DL, Field ME (1999) Subsurface gas offshore of northern California and its link to submarine geomorphology. Mar Geol 154:357–368

Zitellini N, Gràcia E, Matias L, Terrinha P, Abreu MA, DeAlteriis G, Henriet JP, Dañobeitia JJ, Masson DG, Mulde T, Ramella R, Somoza L, Diez S (2009) The quest for the Africa–Eurasia plate boundary west of the Strait of Gibraltar. Earth Planet Sci Lett 280:13–50